JOURNAL OF MATERIALS SCIENCE 31 (1996) 1327–1334

The role of knife sharpness in the slitting of plastic films

C. ARCONA, T. A. DOW
Precision Engineering Center, North Carolina State University, Raleigh, NC 27695, USA

An experimental apparatus has been built that provides information on forces associated with slitting plastic films. The apparatus uses commercially available scissors as an analogue to the counter-rotating knife blades used in industry. Cutting forces were measured using sharp and worn blades at a range of slitting speeds from 0.05–2.5 m s^{-1}. Two important film-base materials were studied; the first was polyethylene terephthalate (PET) and the second, acetal butylate. The influences of speed and knife-edge radius were measured for each base material. For the PET-based film, the forces increased as the blade became dull and decreased with cutting speed. At low speeds, the force required to cut the acetal butylate film was independent of speed, but a sharp decrease in force was observed at a speed that depended upon the blade sharpness. An empirical model for the slitting process has been developed that can estimate the forces measured.

1. Introduction

Many plastic sheet products are processed in wide sheets and slit to the desired width. These products include photographic films and papers, reflective films, copier films and adhesive tapes. Subsequent operations on this slit material are often dependent on the quality of the edge produced. For example, punching the perforations in movie film relies on straight, parallel edges of the film to produce an accurate and repeatable hole size and spacing. In addition to providing a reference for subsequent processes, the slitting operation is also a potential source of debris which can adhere to the surface of the material and cause defects in operation.

The production of straight, consistent film edges requires an understanding of the parameters that affect the quality of the edge. Many tests have been conducted to determine the energy required to tear thin plastic films [1–4]; however, little investigation of plastic-film slitting is available in the literature. Two of the most important variables in the slitting process are knife sharpness and slitting speed. The objective of this paper is to describe the relationship between these variables and the measured cutting force and edge quality.

2. Film-slitting experiments

2.1. Experimental apparatus

The relationships between knife sharpness, cutting speed, cutting forces and film edge quality were investigated using the apparatus sketched in Fig. 1. A pair of scissors was used as a simple analogue to the circular, counter-rotating knives typically used in industrial slitting operations. The particular scissors selected (Fiskars Manufacturing Corporation, Model 9451) have similar sharpnesses, angles between upper and lower blades and spring forces compared to commercial slitting knives. The uniformity of the cutting edges, availability and low cost also made these scissors suitable for developing force data. Fig. 1 shows that the lower blade of the scissors was fixed and the upper blade was closed by pulling the end with a wire wound around an electric motor. The wire passed over a roller mounted on a piezoelectric load cell (Kistler 9251A) and the force to close the scissors and cut the plastic film was measured. The output from the load cell was amplified and displayed on an oscilloscope.

To find the instantaneous magnitude of the blade speed, three optical switches were used. The oscilloscope displayed the signal from these optical switches together with the force. As the upper scissor blade interrupted the light between the emitter and detector of each switch, the output voltage dropped at least 2 V. Thus, the placement of the switches allowed the cutting force at each switch location and variations in average cutting speed over the two 10 mm intervals separating the switches, to be measured. It has been experimentally shown that the cutting speed for the scissors varies by less than 10% over the 20 mm interval of the optical switches. An analysis of this slitting configuration showed that the measured cutting forces would be in error by less than 0.5 N.

Two different plastic film stocks were studied: one was a polyethylene terephthalate (PET)-based film with a thickness of 0.2 mm and the second was acetal butylate-based with a thickness of 0.23 mm. Slitting forces for new and worn blades were measured at cutting speeds of 0.05, 0.25, 0.5, 1.0, 1.5, 2.0 and 2.5 m s^{-1}. The cutting force is assumed to be the force that is perpendicular to the cutting edge of the upper blade. A typical cutting test result is shown in

0022–2461

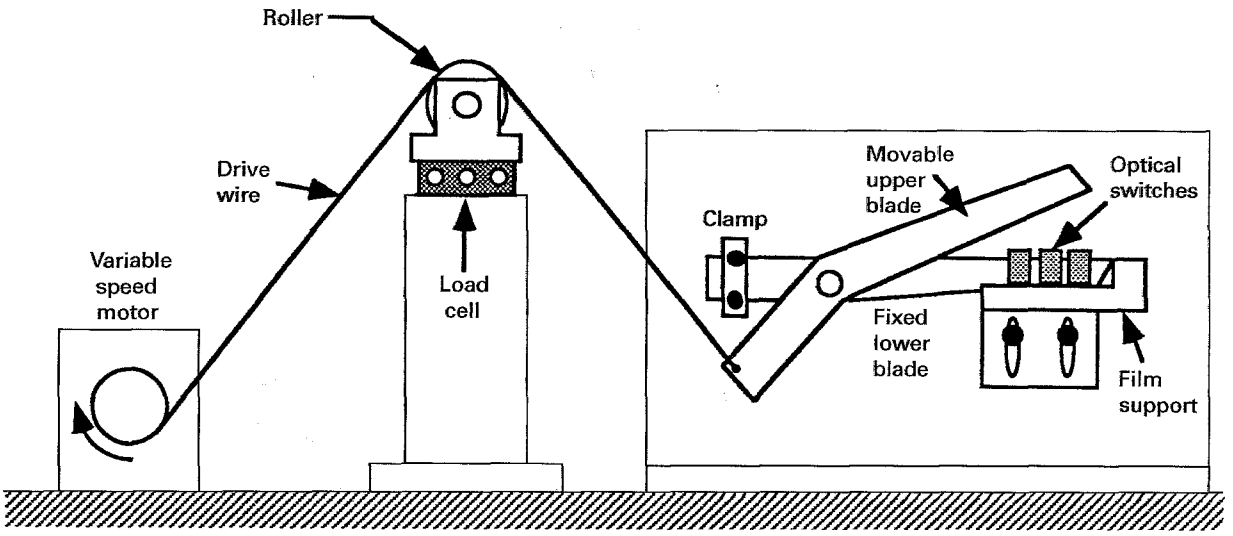

Figure 1 Experimental slitting apparatus.

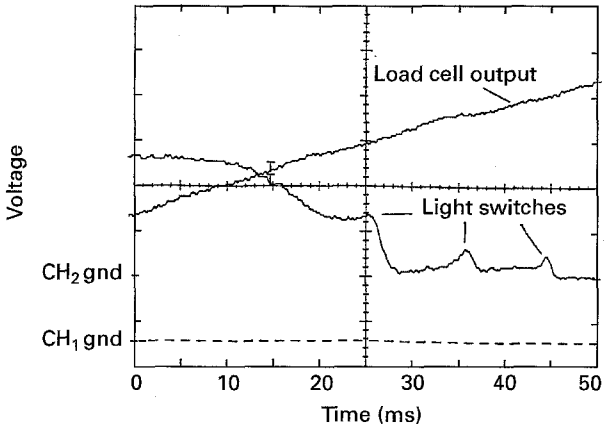

Figure 2 Output for slitting film as displayed on oscilloscope.

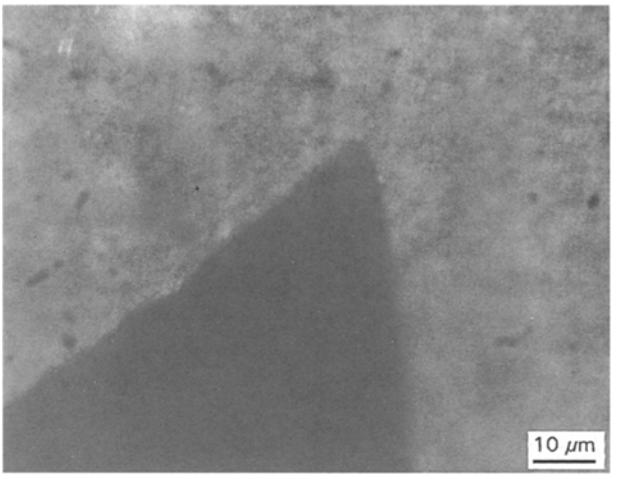

Figure 3 Replicated Fiskars edge profile, X840.

Fig. 2. The results correspond to slitting the acetal butylate-based film at 1 m s^{-1} with the blades having 4.5 μm edge radii. The signals from the load cell and optical switches are indicated in Fig. 2. Each vertical division corresponds to 1 V for channel 1 and 2 V for channel 2. The points at which the three switches were tripped are clearly visible.

2.2. Measuring edge geometry

If the slitting process can be modelled and the optimum knife characteristics determined, it then becomes necessary to have an accurate measurement of the cutting edges of the slitter knives to control the fabrication process. A quick, accurate and non-destructive technique for measuring knife sharpness (i.e. knife-edge radius) was developed wherein an impression of the scissor blade was made using a replica material (vinyl polysiloxane impression material, kit 9400H, manufactured by 3M Corporation). The mould containing the imprint of the blade was then sectioned and viewed in a light microscope. To judge the effectiveness of the method, the scissor blade was sectioned, polished and measured in a scanning electron microscope (SEM). Figs 3 and 4 contain the results of this comparison. Fig. 3 shows a cross-section of the

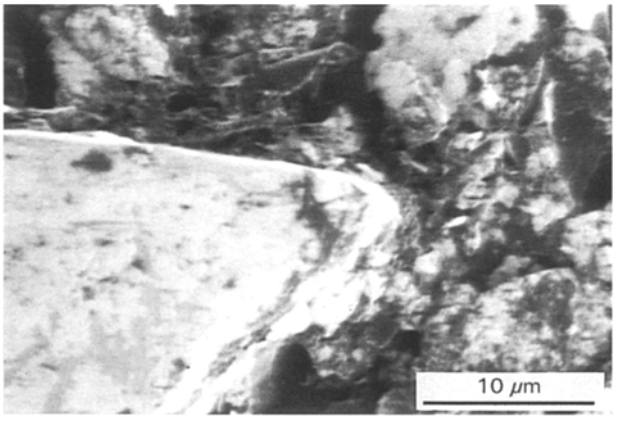

Figure 4 Scanning electron micrograph of the edge, X2100.

impression material taken with the light microscope at a magnification of X840. A circular template was fitted to the void created by the nose of the tool and the edge radius was determined to be 1.7 μm. Two other cross-sections of the mould showed the same edge radius. Using the same circle-fit technique, the radius of the actual cutting edge depicted in the scanning electron micrograph of Fig. 4 was measured as 1.6 μm.

The accuracy and resolution of the replication method proved to be acceptable for measuring the edge radii of the scissor blades.

To develop a worn blade, the scissors were used to cut 600 grit silicon carbide paper. After approximately 100 cuts, the edge radius of the blade used in the slitting experiments changed from 1.9 μm to 4.5 μm. Further cutting (600 additional cuts) produced the largest radius tested which was 8.0 μm.

2.3. Force measurements

Figs 5 and 6 show the cutting force as a function of knife edge radius and slitting speed for the two films. For the sharpest blades (1.9 μm edge radii), the PET film in Fig. 5 showed a nearly linear decrease in cutting force with cutting rate up to a speed of about $1.5\,m\,s^{-1}$ before the force appeared to reach some constant level. Increasing the blade-edge radius raised the force at every cutting speed. The acetal butylate film in Fig. 6 displayed a relatively constant cutting force for cutting speeds less than $2.5\,m\,s^{-1}$ when slitting with the sharpest scissor blades. An abrupt decrease in force occurred between 2.5 and $4\,m\,s^{-1}$. As the edge radius of the blade became dull through intentional wear, the force transition occurred at a lower speed.

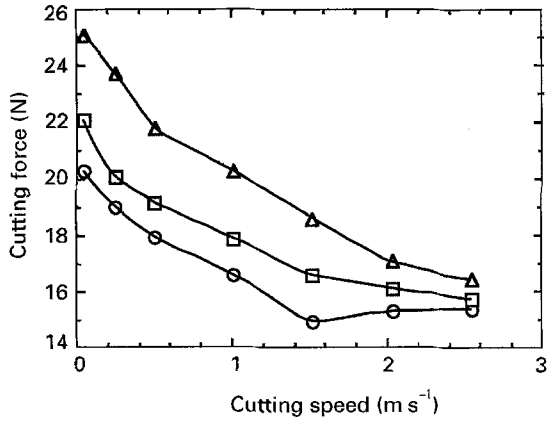

Figure 5 Cutting force versus slitting speed for PET-based film. *R*: (○) 1.9 μm, (□) 4.5 μm, (△) 8.0 μm.

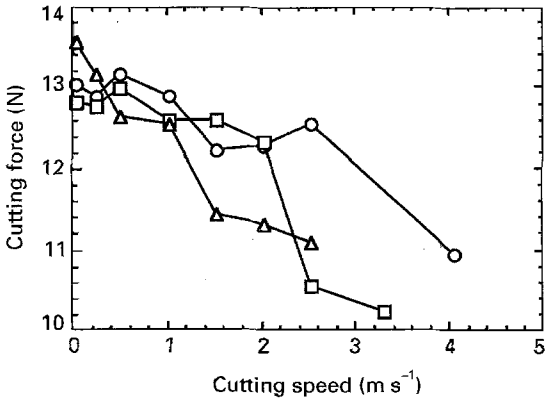

Figure 6 Cutting force versus slitting speed for acetal butylate-based film. *R*: (○) 1.9 μm, (□) 4.5 μm, (△) 8.0 μm.

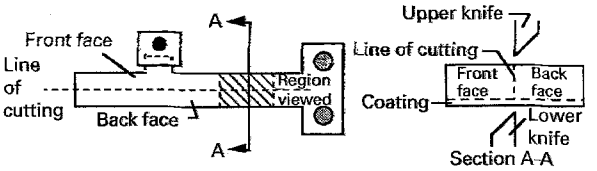

Figure 7 Test piece showing the cross-section investigated.

2.4. Cut-edge measurements

Following the slitting experiments, the film edges were documented using a Zeiss ICM 405 light microscope. The sections of film that were flanked by the optical switches during the cutting tests were removed and positioned on the stage of the microscope. The geometry of the film test pieces is illustrated in Fig. 7. The film surfaces in the plane of slitting as well as those perpendicular to the slit edge were examined. The graduated focus knob of the 500X objective (each division represents a 1 μm motion of the lens) made quantitative documention of the edge profile possible. To facilitate the description of the micrographs, the two halves of the slit film are designated the front and back faces, as indicated in Fig. 7.

3. Discussion

The ductility of the PET-based film and the nature of the slit edges were found to be dependent on the slitting speed. Pictured in Fig. 8 is a PET film edge slit at $50\,mm\,s^{-1}$ with the sharp (1.9 μm edge radii) blades. The magnification of the edge in Fig. 8 is X140. Fig. 8 and the profile sketch in Fig. 9 show that the edge in contact with the angled face of the blade was plastically deformed. (The dimensions in Fig. 9 were obtained from selective focus using the microscope calibration, but the cross-sectional shape of the edge is only approximate.) The upper surface of the edge in Fig. 8 is distorted due to this plastic deformation. In contrast, that part of the edge formed by the lower knife is reflective and fairly smooth. Little debris could be found in these edges formed at a low slitting speed.

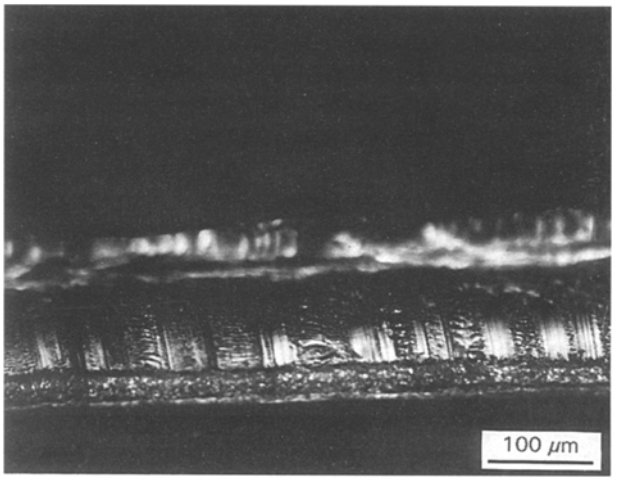

Figure 8 Back face of PET film slit at $50\,mm\,s^{-1}$ with sharp blades, X140.

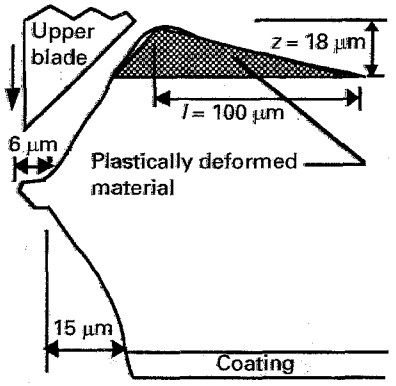

Figure 9 Edge-profile sketch.

The widths of the deformed and smooth regions that comprised the whole of the cross-section of the edges slit at 50 mm s^{-1} decreased as the cutting speed increased. At higher speeds, most of the edge showed a region where layers of PET appeared to have been extruded from the base material. Thread-like debris was present throughout this region. The PET film edge and the edge profile sketch produced by slitting at 2 m s^{-1} with the sharp (1.9 μm edge radius) blades are shown in Figs 10 and 11.

The cross-sectional area of the plastically deformed material (indicated in Fig. 9) was found to vary directly with the slitting force shown in Fig. 5. It was also

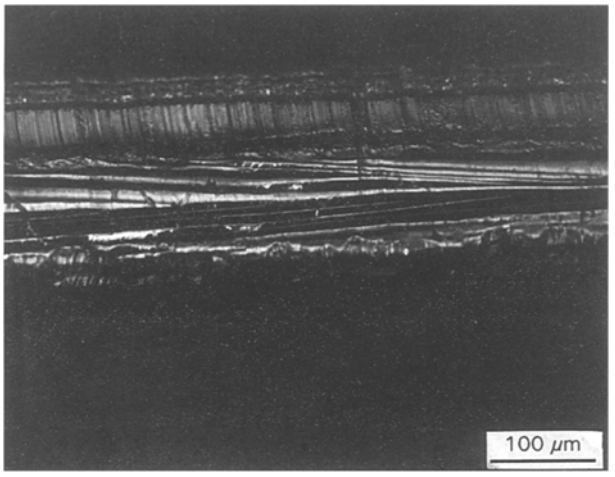

Figure 10 Back face of PET film slit at 2 m s^{-1} with sharp blades, X140.

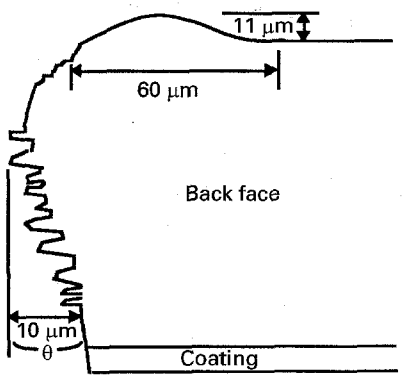

Figure 11 Edge-profile sketch.

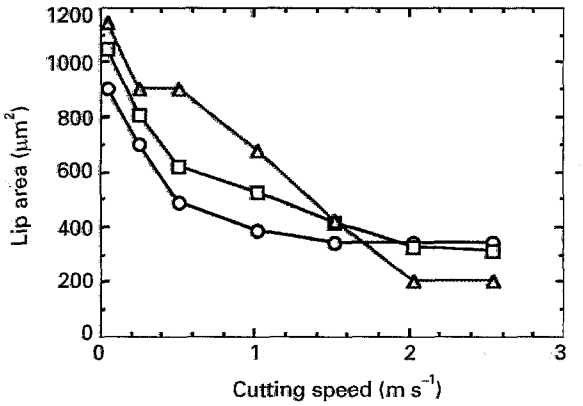

Figure 12 Plastic deformation as a function of slitting speed and blade sharpness for PET film. *R*: (○) 1.9 μm, (□) 4.5 μm, (△) 8.0 μm.

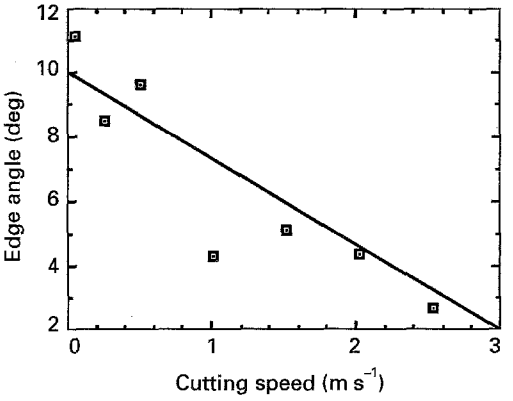

Figure 13 Edge angle for PET film cut with sharp blades.

found that the slitting force became nearly constant when the area of the deformed region became independent of speed. Furthermore, the film failed in a more vertical plane as the slitting speed increased. These results are graphically depicted in Figs 12 and 13. In Fig. 12, the area of the plastically deformed lip is approximated by a triangle of base, *l*, and height, *z*, as shown in Fig. 9. The edge angle, θ, is indicated in Fig. 11. The decrease in distortion of the film edge and the increase in debris produced during slitting suggest that the PET film became less ductile as the cutting rate increased. The type of failure observed for slitting with the sharp blades was also found in the edges produced by blades having 4.5 and 8.0 μm edge radii. Compared to the sharp blades, however, the larger radii of the worn blades produced more damage to the film edge.

In contrast to the ductile PET film, the acetal butylate-based film behaved in a brittle manner under typical slitting conditions. Shown in Fig. 14 is the × 70 micrograph of opposing areas on the two faces of an acetal butylate film sample slit at 50 mm s^{-1} with the sharp blades. The jagged nature of the surfaces indicates brittle fracture. If the faces are rotated about the black line separating their light-coloured emulsion surfaces, they would almost fit together. Preventing a perfect match following this rotation are the crevices that run the lengths of the lower side of the top edge and the upper side of the bottom edge, as shown by Fig. 15. This sketch also indicates that there is no

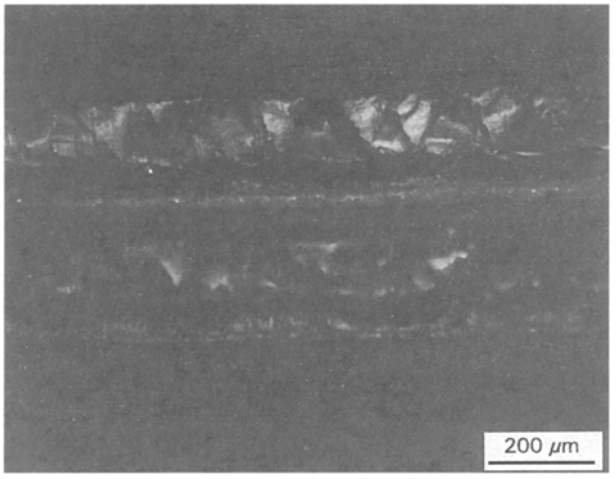

Figure 14 Front and back faces of acetal butylate film slit at 50 mm s^{-1} with sharp blades, X70.

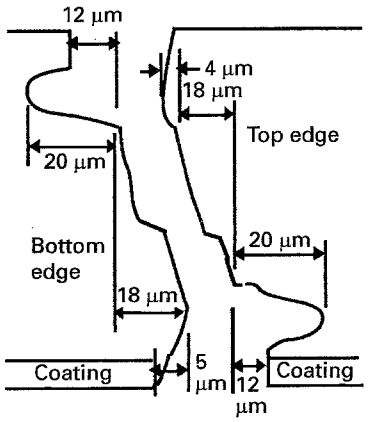

Figure 15 Edge-profile sketch.

raised material on the top surface that touches the angled blade face (compare this edge with that of Fig. 9). Increasing the slitting speed or blade edge radius resulted in the elimination of the ordered fracture seen in Fig. 14. The widths of the crevices in the film edges increased with speed, as did the amount of debris that could be seen in the edges.

At speeds equal to or greater than those required to produce the force transitions of Fig. 6, the edges became relatively square and smooth. The optical microscope showed that the edge angle decreased from about 5° to 3° and the peak-to-valley distortion across the film thickness decreased from about 30 μm to 15 μm as this force transition occurred. Further examination of the edges using a Talystep surface profilometer showed that the average roughness along the length of the film edge decreased from about 2.5 μm to 1.0 μm as the cutting force suddenly decreased with cutting speed. These observations suggest that an abrupt change in the edge profile accompanied the rapid decrease in the slitting force. An explanation for the drop in force could be as follows: as the shear plane becomes vertical and the roughness of the film edges decreases, the area of the surfaces created by the slitting process decreases, and with it, the energy required to produce the new surfaces.

4. Modelling the slitting process

4.1. Cutting-force model for sharp blades

To explain the characteristics of the slit film edges and the associated forces for the different materials, models developed for similar processes were evaluated. Slip line field solutions for cutting and wedge indentation in metals have been developed by Hill [5], Ford [6], Mahtab and Johnson [7] and Johnson *et al.* [8]. These analyses can be used to develop a quantitative explanation for some of the experimental trends measured.

Metal cutting has been modelled as a two-step process: the first is an indentation phase where material along the film surfaces is displaced by pressure from the angled blade faces as the knives penetrate the film. The second phase begins when the transverse tensile stress in the uncut film reaches the yield stress of the material. The remainder of the material is separated through tensile fracture. Hill showed that the cutting force reaches a maximum at the end of the indenting phase [5]. He presented equations for the force as a function of indentation depth for sharp wedges with included angles of less than 45°. The load per unit length of material indented, L, is given by

$$L = 4k(d - c)\tan\theta \quad (1)$$

where k is the shear yield stress, θ is the semi-angle of the wedge ($2\theta < 45°$), d is the material thickness and c is the depth of penetration at the onset of the second phase.

A more general solution for the indentation problem has been developed by Ford [6]. For a sharp tool, the load as a function of the tool geometry and penetration depth is given by

$$L = 4kh(1 + \psi)\sin\theta \quad (2)$$

where L is the load per unit indenting length, k is the shear yield stress of the material and the remaining parameters are indicated in Fig. 16. The relationship between ψ and θ is given by Ford [6].

4.2. PET cutting forces

The force model presented by Ford can be applied to the slitting of the ductile PET-based film. Let θ be the included angle of the scissor blade ($\theta = 60°$) and h is the dimension of the raised material adjacent to the blade, as shown in Fig. 16. The shear yield stress, k, of

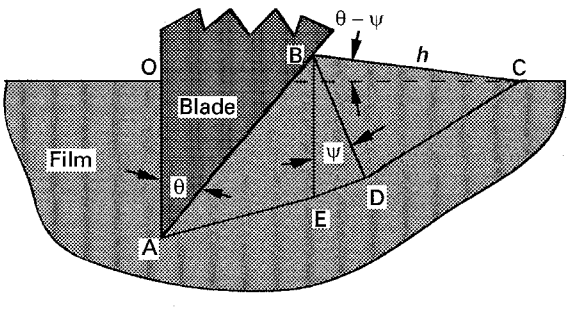

Figure 16 Film parameters used to determine indenting load [6].

PET is taken as one-half of its yield stress in uni-axial tension (k = 34.5 MPa [9]).

Consider an experiment where PET film was slit at 50 mm s^{-1} with the sharp scissor blades (edge radius = 1.9 μm). From the edge profile sketch in Fig. 9, the dimension h is approximately

$$h = (100^2 + 18^2)^{1/2} = 100\ \mu m \quad (3)$$

The angle ψ as given by the geometries in Figs 8 and 15 is $\psi = \theta - \tan^{-1}(18/100) = 50°$, which compares well with the theoretical value given by Ford ($\psi = 52°$, [6]). For slitting, twice the force given by the indentation load equation is expected, because two blades are penetrating the film. For a k value of 34.5 MPa and h of 100 μm, the slitting force is

$$L = 8(34.5\ MPa)(100\ \mu m)[1 + \pi(52°/180°)]\sin 60°$$
$$= 45.6\ kN\,m^{-1} \quad (4)$$

For cutting with sharp blades, the length over which the load L is applied is given approximately by $h/\sin\beta$ where β is the angle between the blades during cutting (13° for the scissors). Thus, the load is distributed over about 450 μm for h = 100 μm so that the slitting force is given by

$$F = 450\ \mu m \times 45.6\ kN\,m^{-1} = 20.5\ N \quad (5)$$

This value is in excellent agreement with the 20.3 N force measured experimentally (see Fig. 5). The correlation of the measured and calculated forces suggests that the experimentally determined slitting forces are the maximum indentation forces occurring at the end of the first phase of the cutting process.

4.2.1. Influence of speed on PET cutting forces

The force model can be modified to include the change in cutting force with speed. Examination of many film edges (such as in Fig. 9) has shown that the height of the plastically deformed material, z, decreases nearly linearly with cutting speed. For slitting with sharp blades, h can be approximated as

$$h = 100 - \frac{100 - 66}{1.5} \times \text{speed}_{\text{cutting}} \quad (6)$$

where h is in μm and cutting speed is in m s^{-1}. This equation holds for cutting speeds less than or equal to 1.5 m s^{-1}. At higher speeds, h is constant and is about 66 μm. For cutting with sharp blades, the dimension over which the load L is applied can be taken as $h/\sin\beta$ where β is the angle between the blades during cutting. An accurate estimate of the cutting force for slitting at high speeds must also incorporate a scale factor to account for the failure of Ford's model under these conditions. This scale factor, SF, is empirical and given by the expression

$$SF = 1 + 0.7\ (\text{cutting speed}/1.5)^{1.5}$$
$$\text{cutting speed} \leqslant 1.5\ m\,s^{-1} \quad (7a)$$

$$SF = 1.7 \quad \text{cutting speed} > 1.5\ m\,s^{-1} \quad (7b)$$

TABLE I Comparison of calculated and measured cutting forces in PET-based film for sharp blades

Slitting speed (m s^{-1})	Calculated force (N)	Measured force (N)	Difference (%)	Scale factor
0.05	19.9	20.3	2.0	1.00
0.25	18.9	19.0	0.55	1.05
0.5	18.1	17.9	1.0	1.13
1.0	16.7	16.6	0.85	1.38
1.5	15.0	14.9	0.74	1.70
2.0	15.0	15.3	1.9	1.70
2.5	15.0	15.4	3.2	1.70

This scale factor could account for the non-linear dependence of the yield stress on the loading rate and the effects of work hardening. The slitting force associated with sharp blades having 60° included angles is then

$$F = [8kh(1 + \psi)\sin\theta]\left(\frac{h}{\sin\beta}\right)SF \times 10^{-6} \quad (8)$$

where F is in N, k is in MPa, h and SF are given in Equations 6 and 7 and ψ = 0.91 radians (52°).

Equation 8 for the slitting force and the experimental results from Fig. 5 yield the entries in Table I. The predicted and measured values are in good agreement. Based on these results, Equation 5 can be used to predict cutting forces associated with sharp blades having included angles of 60° for a wide range of speeds.

4.2.2. Influence of blade sharpness on PET cutting forces

Further modifications of the force model (Equation 8) can take into account the variation in slitting force with blade-edge radius. For slitting at speeds less than 1.5 m s^{-1}, the cutting force varies linearly with blade-edge radius, as shown by Fig. 17. Fig. 17 also demonstrates that the slope of the cutting force as a function of blade sharpness is nearly constant.

The cutting force as a function of both slitting speed and edge radius can be calculated by modifying Equation 8 with the information in Fig. 17. Taking the average slope of the lines in Fig. 17 as 0.685 N μm^{-1}

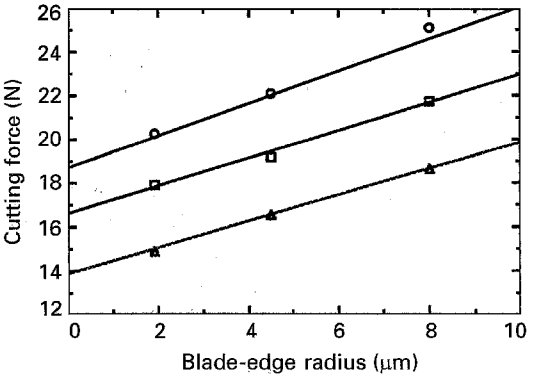

Figure 17 Cutting force versus blade-edge radius for PET film at several speeds: (○) 0.05 m s^{-1}, (□) 0.5 m s^{-1}, (△) 15 m s^{-1}.

TABLE II Comparison of calculated and measured cutting forces in PET-based film for 4.5 and 8.0 μm edge radius blades

Speed ($m s^{-1}$)	Force (N) from Eq. 9, $R = 4.5$ μm	Measured force (N), $R = 4.5$ μm	Difference (%)	Force (N) from Eq. 9, $R = 8.0$ μm	Measured force (N), $R = 8.0$ μm	Difference (%)
0.05	21.7	22.1	1.8	24.1	25.1	4.0
0.25	20.7	20.1	3.0	23.1	23.7	2.5
0.50	19.9	19.2	3.6	22.3	21.8	2.3
1.0	18.5	17.9	3.4	20.9	20.3	3.0
1.5	16.8	16.5	1.8	19.2	18.6	3.2

and applying a point-slope equation with the result of Equation 8 acting as the intercept, yields the following force equation

$$F = [8kh(1 + \psi)\sin\theta]\left(\frac{h}{\sin\beta}\right)SF \times 10^{-6} + 0.658(R - 1.9) \quad (9)$$

where R is the blade-edge radius in μm. This equation is developed for slitting speeds less than 1.5 $m s^{-1}$ and blade edge radii between 1.9 and 8.0 μm. A comparison of slitting forces measured with the dull blades (4.5 and 8.0 μm edge radii) and those calculated using Equation 9 is given in Table II. Excellent agreement between measured and predicted forces was obtained.

4.3. Acetal butylate cutting forces

The load equation presented by Ford cannot be applied to the slitting of the brittle acetal butylate-based film because there is no obvious plastic deformation. Without the lip of raised material (see Fig. 15), it is not possible to estimate the parameter h. Fig. 18, however, suggests that the two phases of cutting do occur in the slit samples. Fig. 18 shows the front face of the acetal butylate film sample cut slowly with sharp scissors. The edge pictured was created by cutting slowly (~ 50 mm s^{-1}) with hand-held scissors having blades with 1.9 μm edge radii. A steel rod was held against the film with its axis perpendicular to the line of cutting so that the closing blades stopped suddenly when the rod was struck. The film was then slowly torn in the direction of the line of cutting. The sample was mounted so that the cut/tear interface could be viewed in a light microscope. The point at which indentation ceased and separation began is visible in the photo and is also indicated in Fig. 19. Applying Hill's force equation (Equation 1) with $k = 20.7$ MPa [9], $\theta = 60°$, $d - c = 0.15$ mm (0.075 mm indentation depth from Fig. 18) yields $L = 43.0$ N mm^{-1}. From Fig. 18, the contact length during indentation, l, is about 0.31 mm. The calculated force is then 13.3 N, which compares favourably to the 12.9 N force determined experimentally. Although Hill's force equation was developed for indenting ductile materials with blade angles that are less than 45°, it provides a reasonable estimate of the slitting force for the brittle acetal butylate film with blades having 60° included angles. Thus, the measured slitting force corresponds to the maximum indentation force, as in the case of slitting the ductile PET-based film.

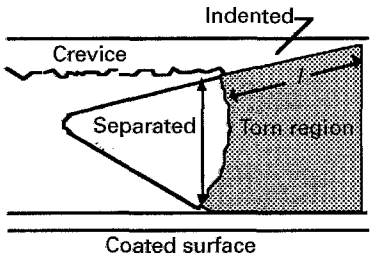

Figure 19 Cut/tear interface sketch.

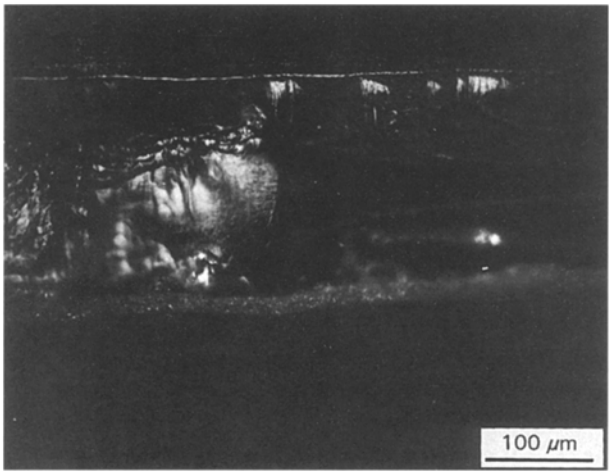

Figure 18 Cut/tear interface in acetal butylate film, sharp blades, slow speed, X140.

5. Conclusion

Techniques for measuring a cutting tool with less than a 10 μm edge radius are limited to scanning electron microscopy, probing the cutting edge with a tip of known geometry, and replication methods. The time-consuming and expensive nature of the SEM technique and the high contact stresses associated with the mechanical technique make these methods unattractive for quantifying the many knives of a commercial slitting line. Replication techniques combined with optical microscopy represent a quick, accurate and non-contact mode of knife-edge measuring.

The response of the PET-based film and the acetal butylate-based films to varying knife sharpness and slitting speed were very different. At low slitting speeds, the PET film was subject to significant plastic

deformation. The ductility of the film and cross-sectional area of the plastically deformed regions along the film surfaces decreased with increasing cutting rate. The slitting force was determined to vary directly with the amount of plastic deformation. In contrast, the acetal butylate film behaved in a brittle manner under typical slitting conditions. From investigation of the slit edges using an optical microscope, it was also observed that an increase in the edge radii of the blades or the slitting speed generally resulted in a greater amount of debris produced by the process. Furthermore, it was found that slip-line field solutions to wedge indentation in metals can be used to model the slitting of polymer films under some conditions.

Acknowledgements

The authors would like to thank the sponsors of the Precision Engineering Center including Kodak, Texas Instruments, 3M, Los Alamos National Labs, Livermore National Labs, Oak Ridge National Labs, Rank Taylor Hobson and IBM, for supporting this work.

References

1. D. S. CHIU, A. N. GENT and J. R. WHITE, *J. Mater. Sci.* **19** (1984) 2622.
2. J. A. HINKLEY and C. A. HOOGSTRATEN, *ibid.* **22** (1987) 4422.
3. A. N. GENT and J. JEONG, *ibid.* **21** (1986) 355.
4. G. E. ANDERTON and L. R. G. TRELOAR, *ibid.* **22** (1987) 562.
5. R. HILL, *J. Mech. Phys. Solids* **1** (1953) 265.
6. H. FORD, "Advanced Mechanics of Materials" (Wiley, New York, 1963).
7. F. U. MAHTAB and W. JOHNSON, *Int. J. Machine Tool Design* **2** (1962) 335.
8. W. JOHNSON, R. SOWERBY and R. D. VENTER, "Plane Strain Slip Line Fields for Metal Deformation Processes" (Pergamon Press, Oxford, 1982).
9. I. RUBIN (ed.) "Handbook of Plastic Materials and Technology" (Wiley, New York, 1990).

Received 31 October 1994
and accepted 16 August 1995